

A Fully Integrated Dual-Band WLP CMOS Power Amplifier for 802.11n WLAN Applications

Seungjun Baek¹ · Hyunjin Ahn¹ · Hyunsik Ryu¹ · Ilku Nam¹ · Deokgi An² · Doo-Hyouk Choi² ·
Mun-Sub Byun² · Minsu Jeong² · Bo-Eun Kim² · Ockgoo Lee^{1,*}

Abstract

A fully integrated dual-band CMOS power amplifier (PA) is developed for 802.11n WLAN applications using wafer-level package (WLP) technology. This paper presents a detailed design for the optimal impedance of dual-band PA (2 GHz/5 GHz PA) output transformers with low loss, which is provided by using 2:2 and 2:1 output transformers for the 2 GHz PA and the 5 GHz PA, respectively. In addition, several design issues in the dual-band PA design using WLP technology are addressed, and a design method is proposed. All considerations for the design of dual-band WLP PA are fully reflected in the design procedure. The 2 GHz WLP CMOS PA produces a saturated power of 26.3 dBm with a peak power-added efficiency (PAE) of 32.9%. The 5 GHz WLP CMOS PA produces a saturated power of 24.7 dBm with a PAE of 22.2%. The PA is tested using an 802.11n signal, which satisfies the stringent error vector magnitude (EVM) and mask requirements. It achieved an EVM of -28 dB at an output power of 19.5 dBm with a PAE of 13.1% at 2.45 GHz and an EVM of -28 dB at an output power of 18.1 dBm with a PAE of 8.9% at 5.8 GHz.

Key Words: CMOS, Integrated Circuit, Power Amplifier, Transformer, WLAN.

I. INTRODUCTION

The rapid development of handheld devices has necessitated the transmission and reception of high data-rate signals. Despite the developments in wireless communication technologies, the design of CMOS power amplifiers (PA) continues to pose challenges in the design of wireless transceivers because of the low breakdown voltage in CMOS devices, the no-substrate via-hole in the CMOS process, and the low quality of the passive components. In addition, in WLAN applications, especially those meeting the IEEE 802.11n standard, a highly linear PA is required because of the high peak-to-average power ratio (PAPR) and the wide data bandwidth signal. Therefore, PAs

are required to operate in a large back-off point from the in a saturation power region, resulting in decreased efficiency [1]. Hence, the design of WLAN PAs using CMOS technology is a challenging task.

Current communication standards require that PAs support dual or multi-bands. Therefore, the demand for dual-band PAs has increased. In 802.11n applications, 2 GHz and 5 GHz bands must be supported. In dual-band operation, the design of the output transformer is crucial because it must provide optimal impedance with low loss performance. However, no detailed design for the optimization of dual-band PA (2 GHz/5 GHz PA) output transformers has been reported. In wafer-level package (WLP) technology, an integrated circuit is used as the

Manuscript received October 5, 2016 ; Revised December 12, 2016 ; Accepted December 30, 2016. (ID No. 20161005-034J)

¹School of Electronic and Computer Engineering, Pusan National University, Busan, Korea.

²RAONTECH Inc., Seongnam, Korea.

*Corresponding Author: Ockgoo Lee (e-mail: olee@pusan.ac.kr)

This is an Open-Access article distributed under the terms of the Creative Commons Attribution Non-Commercial License (<http://creativecommons.org/licenses/by-nc/3.0>) which permits unrestricted non-commercial use, distribution, and reproduction in any medium, provided the original work is properly cited.

© Copyright The Korean Institute of Electromagnetic Engineering and Science. All Rights Reserved.

wafer level. WLP is essentially a true chip-scale package technology because the resulting package is almost the same size as the die [2]. Because WLP is intrinsically a chip-size package, its primary advantage is its small form factor. Another advantage is its low packaging cost compared to die-level packaging [3]. WLP technology also allows the chip to be reliably attached directly to a printed circuit board (PCB) [4]. However, unlike other packaging methods, it is difficult to design a dual-band PA in a compact die area using WLP technology because there are several limitations in the usage of WLP technology in RF PA designs. Without proper design considerations, the required die area is greatly increased because of the minimum distance rule between the balls and their large diameter. Although a dual-band PA using WLP technology was developed in [5], the considerations and details related to the design of a dual-band PA using WLP technology have not been addressed.

In this work, several design issues in a dual-band PA using WLP technology are addressed and a design method is proposed. In addition, a detailed design for the optimal impedance of dual-band PA (2 GHz/5 GHz PA) output transformers with low loss is presented. In the optimal dual-band operation presented here, the selection of the number of turns in the primary and secondary windings of the output transformers is investigated to provide optimal impedance. We design and implement a fully integrated dual-band CMOS PA for 802.11n applications using WLP technology. The fully integrated 2 GHz CMOS PA exhibits a 19.5-dBm output power and a PAE of 13.1% at the -28 dB error vector magnitude (EVM) point; the 5 GHz CMOS PA achieves an 18.1-dBm output power and a PAE of 8.9% at the -28 dB EVM point.

II. OUTPUT TRANSFORMER DESIGN FOR THE DUAL-BAND CMOS PA

The output transformer is a major component affecting the overall performance of the PA. In designing a highly efficient linear PA, the selection of the optimal impedance is crucial. In the initial design stage, load-pull simulations are typically performed to find the optimal region of the input impedance in the transformers (Z_{IN}). Therefore, an output transformer is required to provide the corresponding optimal impedance region with low loss performance.

Fig. 1(a) depicts the layouts of 1:2 and 2:2 transformers. The equivalent model of a magnetic-coupled transformer is shown in Fig. 1(b). L_1 is the net inductance of the primary winding and L_2 is the net inductance of the secondary winding. R_1 and R_2 are the net resistances of the primary and secondary windings, respectively. Considering the effect of the voltage induced through mutual coupling,

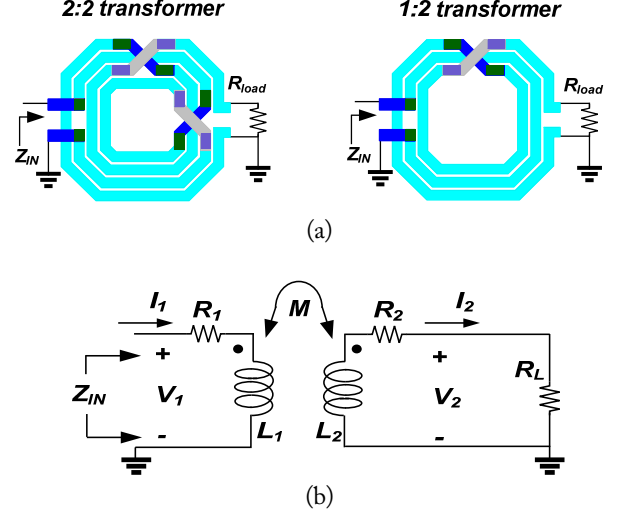


Fig. 1. (a) Exemplary layouts for 2:2 and 1:2 transformers, (b) equivalent circuit model for a magnetic-coupled transformer.

$$\begin{bmatrix} V_1 \\ V_2 \end{bmatrix} = \begin{bmatrix} R_1 + j\omega L_1 & -j\omega M \\ j\omega M & -R_2 - j\omega L_2 \end{bmatrix} \begin{bmatrix} I_1 \\ I_2 \end{bmatrix} \quad (1)$$

$$M = k \cdot \sqrt{L_1 L_2} \\ V_1 = (R_1 + j\omega L_1)I_1 - j\omega M I_2 \quad (2)$$

$$V_2 = j\omega M I_1 - (R_2 + j\omega L_2)I_2 \\ = R_{load} I_2 \quad (3)$$

where M represents the mutual inductance between the primary and secondary windings. Z_{IN} is the input impedance of the transformer, and R_{load} is the output impedance of the transformer. R_{load} is typically 50Ω . From (2) and (3), Z_{IN} is given by

$$Z_{IN} = \frac{V_1}{I_1} = R_{IN} + jX_{IN} \\ = R_1 + j\omega L_1 + \frac{\omega^2 M^2}{R_{load} + R_2 + j\omega L_2} \quad (4)$$

$$R_{IN} = R_1 + \frac{\omega^2 k^2 L_1 L_2 (R_{load} + R_2)}{(R_{load} + R_2)^2 + \omega^2 L_2^2} \quad (5)$$

Because the R_2 and L_2 of the 1:2 transformer almost equal those of the 2:2 transformer, the differences in R_1 and L_1 determine the input impedance (R_{IN}) provided by the transformer. Because the R_1 and L_1 of the 1:2 transformer are lower than those of the 2:2 transformer, the 1:2 transformer provides a low R_{IN} compared to the 2:2 transformer. Fig. 2 illustrates the simulated R_{IN} and the minimum insertion loss. The minimum insertion loss, which is the inverse of the maximum available gain, was previously used to evaluate the passive loss performance [6]. The two transformers are the same size. A $30\text{-}\mu\text{m}$ metal width is used in the transformer design. Both transformers have simi-

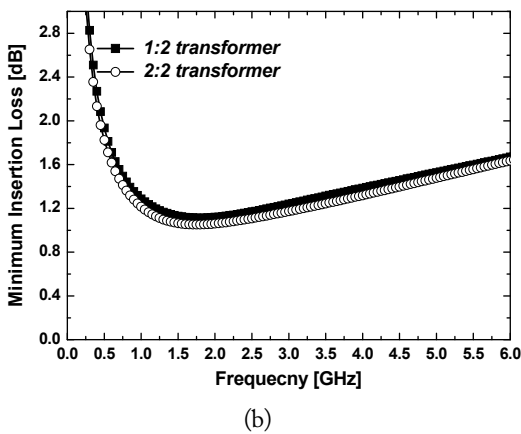
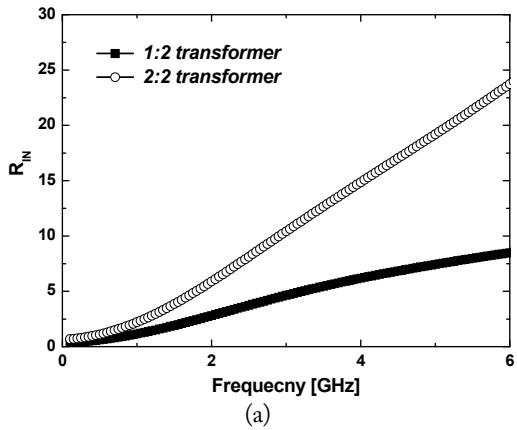


Fig. 2. (a) Simulated R_{IN} of the 2:2 and 1:2 transformers, (b) simulated minimum insertion loss of the 2:2 and 1:2 transformers.

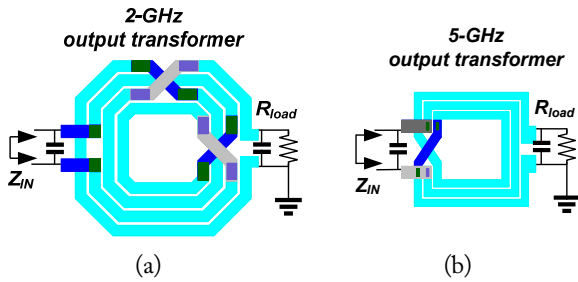


Fig. 3. (a) 2 GHz PA output transformer with input and output capacitors, (b) 5 GHz PA output transformer with input and output capacitors.

lar minimum insertion losses. Fig. 2(a) shows that the R_{IN} of the 1:2 transformer is lower than that of the 2:2 transformer. The power generated by the device is inversely proportional to R_{IN} [7]. Therefore, the power generated by the 1:2 transformer is higher. In a 5 GHz PA operation, the passive loss is usually higher, and its operation has a larger impact on the device's parasitic structure than the 2 GHz operation has. Thus, the power generated by the device should be higher to compensate for the effects of high frequency. In addition, the load-pull simulations validated that the optimum region of Z_{IN} in the 5 GHz PA

output transformer was lower than that in the 2 GHz PA output transformer. Therefore, in this design, the 2:2 transformer was selected for the 2 GHz PA operation [8], and the 1:2 transformer was chosen for the 5 GHz PA operation.

The layouts of the output transformer in each band are shown in Fig. 3. The sizes of the transformers are optimized for each target frequency. The output transformers are designed with a 3.4- μm Cu metal layer. However, EM simulations, optimum metal width, spacing, and the size are selected for both 2 GHz and 5 GHz PA output transformers. The windings of the 2:2 transformer used in the 2 GHz PA are 30 μm wide and

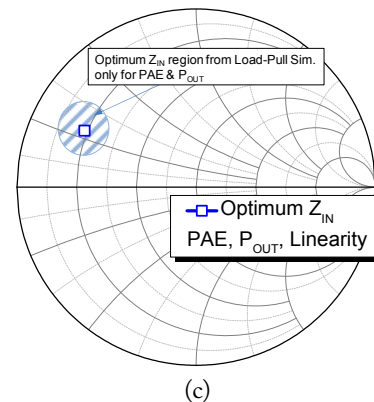
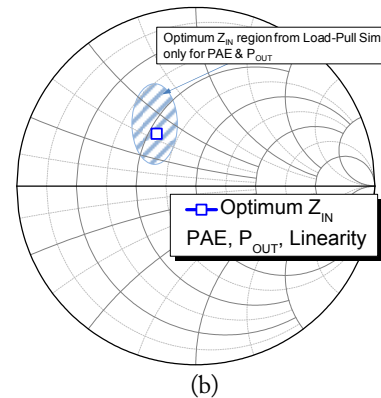
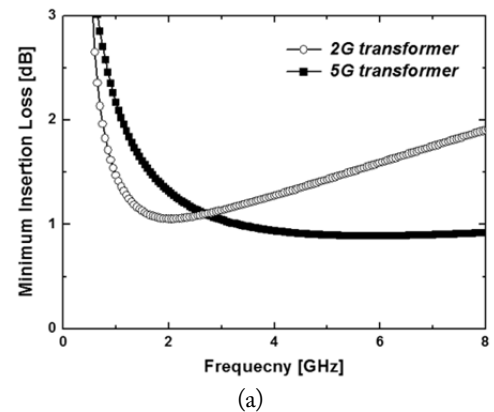


Fig. 4. (a) Simulated minimum insertion loss of the 2-GHz and 5-GHz output transformers, (b) optimum Z_{IN} of 2 GHz PA output transformer, (c) optimum Z_{IN} of 5 GHz PA output transformer.

spaced at 10- μm intervals. The windings of the 1:2 transformer used in the 5 GHz PA are 15 μm wide and spaced at 5- μm intervals. Typically, for high target frequencies, the optimal size for maximizing passive efficiency is smaller in on-chip transformer designs. Increasing the size of the transformer increases the Q of the transformer at lower frequencies, while it can degrade the Q of the transformer at higher frequencies mainly because of the large coupling between the transformer and the lossy substrate. Therefore, the optimized size of the 5 GHz output transformer is much smaller than that of the 2 GHz output transformer. The size of the 2:2 transformer is 495 $\mu\text{m} \times 495 \mu\text{m}$, whereas that of the 1:2 transformer is 235 $\mu\text{m} \times 235 \mu\text{m}$. Fig. 4(a) shows the minimum insertion loss in the output transformers. With the proper section of transformer size, the peak of the minimum insertion loss is located on the target frequencies. When each transformer is plugged into the power stage circuit, input and output capacitors are added in parallel, as shown in Fig. 3, to provide the optimal performances of not only PAE and output power but also linearity. Through a careful process of the iteration of the total circuit simulation to maximize overall performance, the optimal Z_{IN} of the 2-GHz/5-GHz PA output transformers are selected, as shown in Fig. 4(b) and (c).

III. WLAN DUAL-BAND WLP PA DESIGN

Among the most recent packaging solutions, WLP is the preferred method because the packaging size is small and the required cost is low. Careful considerations are required for a dual-band PA design using WLP technology in order to minimize the required die area. To save the die area, a method placing an active device or passive transformers under the WLP balls can be considered. Placing active devices that operate at low frequency, such as digital circuits, under WLP balls may not cause any difference in performance. However, placing active devices or passive transformers that operate at 2 GHz or 5 GHz frequency ranges causes the performance degradations because of the electric and magnetic coupling between the active devices and the WLP balls. In particular, the passive transformer should be kept outside the area of the balls in order to minimize their impact. Because the increasing distance between the designed transformer and the balls also increases the required die area, the selection of the proper distance is importance to save the die area without causing the performance to degrade. Based on EM simulations, a minimum distance of 40- μm between the transformers and balls was chosen in this work.

Fig. 5 shows the schematic of the PAs. Both the 2 GHz and the 5 GHz PAs have differential amplifiers with a cascode structure. To achieve a high gain, the 2 GHz PA has two stages (i.e., the driver stage and the power stage), and the 5 GHz PA has three stages (i.e., driver stage 1, driver stage 2, and the power

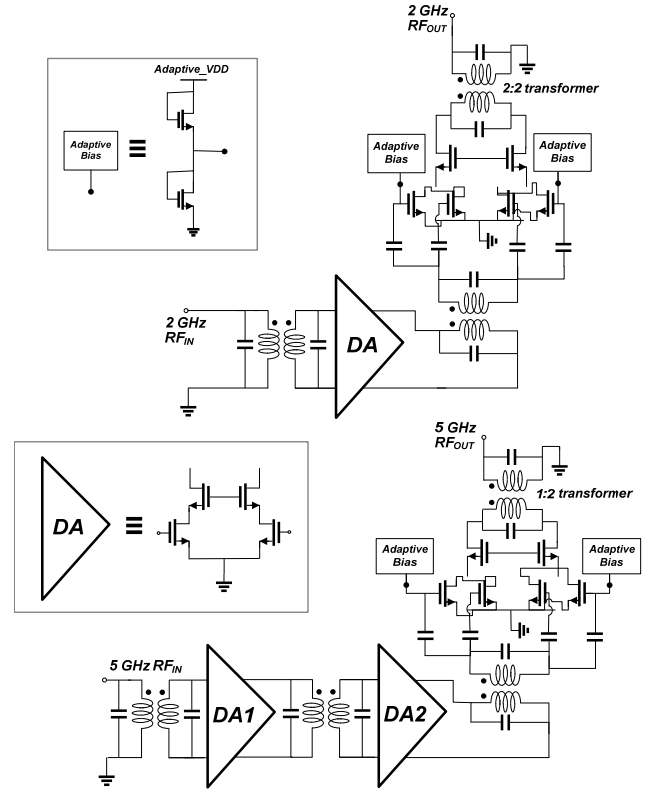


Fig. 5. Schematic of the fully integrated 2 GHz and 5 GHz CMOS PA.

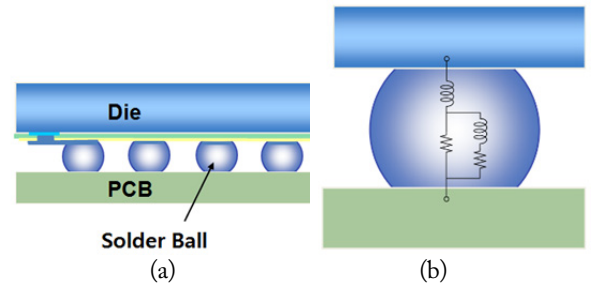


Fig. 6. (a) Typical WLP ball structure with PCB and die, (b) equivalent WLP ball model.

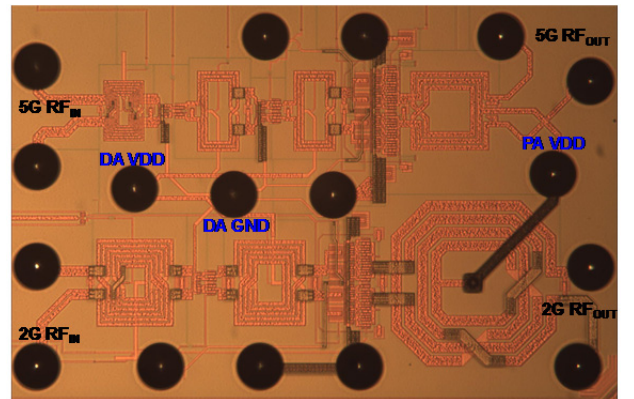


Fig. 7. Die photograph of the fabricated dual-band PA.

stage). An adaptive bias circuit is added to improve the EVM performance of the 2 GHz and 5 GHz PAs [9]. Fig. 6(a) shows

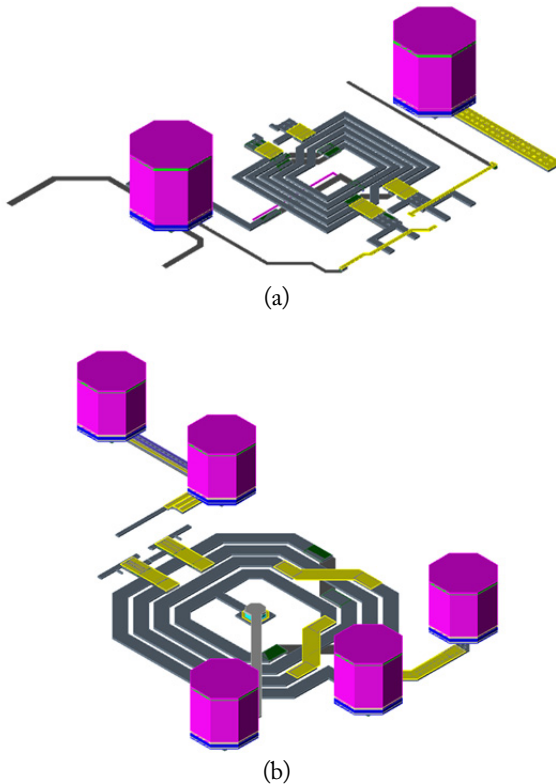


Fig. 8. (a) Full EM model for 2-GHz inter-stage including wafer-level package (WLP) balls and routings, (b) full EM model for 2-GHz output stage including WLP balls and routings.

a WLP structure with PCB and die. In the initial design stage, its equivalent ball model is used for total circuit simulations. Fig. 6(b) shows the equivalent WLP ball model. Because the diameter of ball is $130\ \mu\text{m}$, and the minimum distance between two balls is $300\ \mu\text{m}$ in this work, the increased number of balls increases the required die area. Thus, the number of balls required in the dual-band PA design should be reduced by sharing. Fig. 7 shows a die photograph of the fabricated dual-band PA. As shown in Fig. 7, the power stages (2G PA) in the 2 GHz PA and the power stages (5G PA) in the 5 GHz PA share the PA VDD ball. In addition, the driver stage (2G DA) in the 2 GHz PA and the driver stage 1/driver stage 2 (5G DA1/DA2) in the 5 GHz PA share the DA VDD ball. In the driver stage design, the DA GND ball is also shared by 2G DA and 5G DA1/DA2. In this case, the performance is significantly compromised by the presence of connection routings. The parasitic effects in the connection routings and the balls are caused mostly by magnetic and capacitive coupling. Therefore, proper EM modeling is required to capture these couplings. Through full EM simulations, all transformers (input/inter-stage/output transformer) were re-modeled, including the surrounding balls and the closed signal/VDD/ground routings. All coupling effects are captured and included in the circuit simulations. Fig. 8 shows examples of a 2-GHz inter-stage/output-stage transformer,

including the WLP balls and routings applied to capture interactions and parasitic effects.

IV. MEASUREMENT RESULTS

The fully integrated 802.11n CMOS PA was fabricated using a standard process of 65 nm CMOS. The size of the chip, including the test pads, was $2.04\ \text{mm}^2$, as shown in Fig. 7. During the measurement procedure, the losses in the PCB trace were carefully de-embedded, but the pad and bond wire losses were not de-embedded. Fig. 9(a) shows the measured gain and the PAE versus the output power at 2.45 GHz. The input signal was a single-tone continuous wave (CW) at 2.45 GHz. With a 3.3-V supply, the measurement results showed a 27.7 dB power gain. The saturated output power was approximately 26.3 dBm with a 32.9% PAE.

Fig. 9(b) shows the measured EVM and PAE versus the output power at 2.45 GHz using an MCS7 802.11n signal (64-QAM 65 Mbps with a 20-MHz BW and 9.6 dB PAPR). In the 802.11n standard, the specification for EVM is typically required to be below $-28\ \text{dB}$. At the $-25\ \text{dB}$ EVM point, the output power was 20.3 dBm with a 15% PAE. At the $-28\ \text{dB}$ EVM point, the output power was 19.5 dBm with a 13.1%

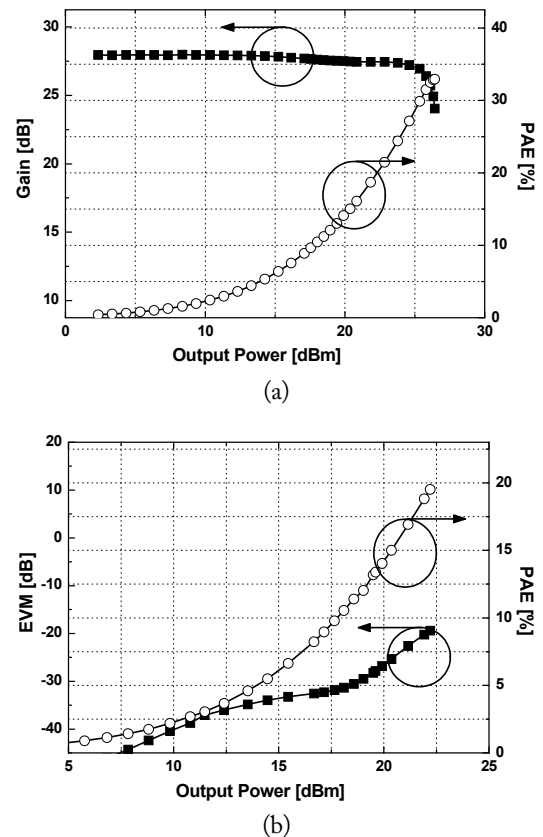


Fig. 9. (a) Measured gain and PAE for the 2.45 GHz continuous wave signal, (b) measured EVM and PAE for the 802.11n signal at 2.45 GHz.

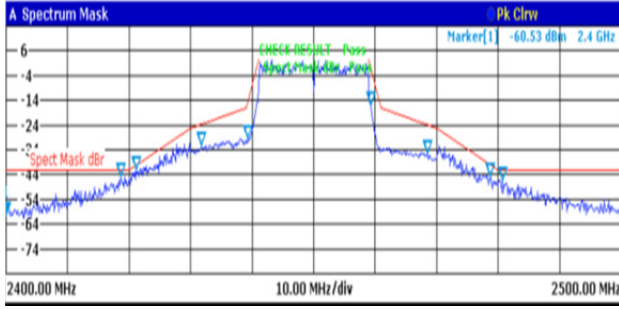
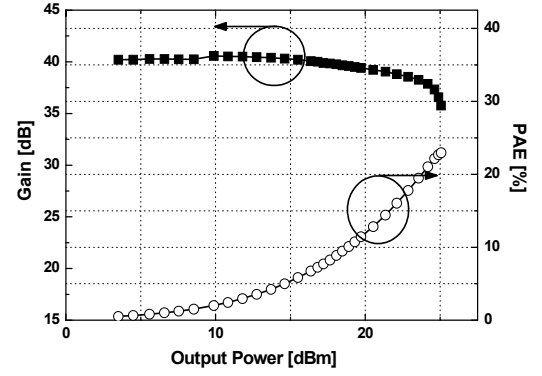
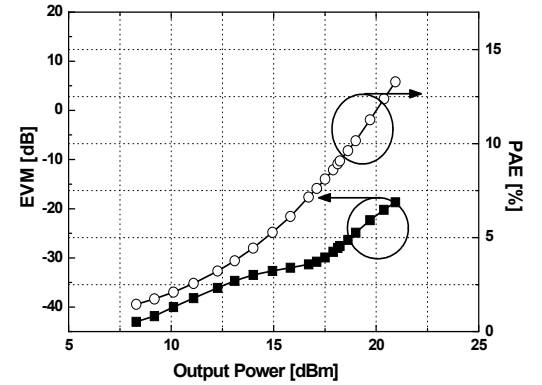


Fig. 10. Output spectrum of the PA for a 2.45 GHz 802.11n signal at a P_{OUT} of 19.5 dBm.

PAE. The measured output spectrum for the 2.45 GHz MCS7 802.11n signal is shown in Fig. 10. The output spectrum satisfied the mask specification at an output power of 19.5 dBm with a -28 dB EVM. Fig. 11(a) shows the measured gain and PAE versus the output power at 5.8 GHz. The input signal was a CW of 5.8 GHz. With a 3.3 V supply, the measured gain was approximately 40 dB. The saturated output power was 24.7 dBm with a 22.2% PAE. Fig. 11(b) shows the measured EVM and PAE versus the output power at 5.8 GHz using an MCS7 802.11n signal (64-QAM 65 Mbps with a 20-MHz BW and 9.6 dB PAPR). At the -25 dB EVM point, the output power was 18.8 dBm with a 9.8% PAE. At the -28 dB EVM point, the output power was 18.1 dBm with an 8.9% PAE. The measured output spectrum for a 5.8 GHz MCS7 802.11n signal is shown in Fig. 12. The output spectrum satisfied the mask specification at an output power of 18.1 dBm with a -28 dB EVM. Table 1 shows the comparison with a recently reported dual-band 802.11b/g/a CMOS PA. The PAPR of the 802.11n MCS7 in HT20 was 0.5 dB higher than that of the 802.11g or the 802.11a [11]. Therefore, the PA that uses an 802.11n signal should operate more linearly than the PA that uses an 802.11g/a signal. Without applying predistortion, the performance of the implemented 802.11n CMOS PA was comparable to those re-



(a)



(b)

Fig. 11. (a) Measured gain and PAE for the 5.8 GHz continuous wave signal, (b) measured EVM and PAE for the 802.11n signal at 5.8 GHz.

ported in [5, 10].

V. CONCLUSION

In this work, we developed a fully integrated dual-band CMOS PA for 802.11n WLAN applications using WLP technology. The output transformer structures were investigated and

Table 1. Comparison with recently reported WLAN WLP CMOS PAs

Ref.	Technology	WLP	Signal	P_{sat} (dBm)		-28 dB EVM			
						P_{OUT} (dBm)		PAE (%)	
				2 GHz	5 GHz	2 GHz	5 GHz	2 GHz	5 GHz
[5]	45 nm CMOS	Yes	802.11b/g/a (54 Mbps)	29	26	20.8 ^a	17.3 ^a	N/A	
[10]	55 nm CMOS	No	802.11 LG54M (54 Mbps)	27	26	20.8 ^a	18.4 ^a	N/A	
This work	65 nm CMOS	Yes	802.11n (65 Mbps)	26.3	24.7	19.5	18.1	13.1	8.9

PA = power amplifier, WLP = wafer-level package, EVM = error vector magnitude.

^aWith predistortion.

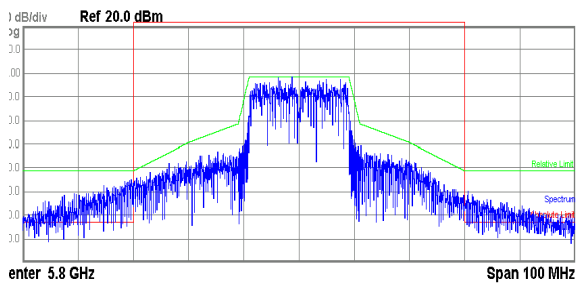


Fig. 12. Output spectrum of the PA for a 5.8 GHz 802.11n signal at a P_{OUT} of 18.1 dBm.

optimized for optimal dual-band operations. A 2:2 output transformer was chosen as the output transformer for the 2 GHz PA, and a 1:2 output transformer was chosen as the output transformer for the 5 GHz PA. The 2 GHz CMOS PA produced a saturated output power of 26.3 dBm with a 32.9% PAE. The 2 GHz PA achieved -28 dB EVM at an output power of 19.5 dBm with a 13.1% PAE. It also satisfied the mask requirements without the need to apply predistortion. The 5 GHz CMOS PA produced a saturated output power of 24.7 dBm with a 22.2% PAE. The 5 GHz PA achieved -28 dB EVM at an output power of 18.1 dBm with an 8.9% PAE. It also satisfied the mask requirements without the need to apply predistortion.

This work was supported by a 2-year Research Grant of Pusan National University.

REFERENCES

- [1] S. C. Cripps, *RF Power Amplifiers for Wireless Communication*. Boston, MA: Artech House, 1999, pp. 246-248.
- [2] X. Fan and Q. Han, "Reliability challenges and design considerations for wafer-level packages," in *Proceedings of International Conference on Electronic Packaging Technology & High Density Packaging (ICEPT-HDP)*, Shanghai, China, 2008, pp. 1-6.
- [3] J. J. Reche and D. H. Kim, "Wafer level packaging having bump-on-polymer structure," *Microelectronics Reliability*, vol. 43, no. 6, pp. 879-894, 2003.
- [4] B. Rogers, C. Scanlan, and T. Olson, "Implementation of a fully molded fan-out packaging technology," in *Proceedings of 10th International Wafer-Level Packaging Conference (IWLPC)*, San Jose, CA, 2013, pp. 1-6.
- [5] R. Kumar, T. Krishnaswamy, G. Rajendran, D. Sahu, A. Sivadas, M. Nandigam, et al, "A fully integrated 2×2 b/g and 1×2 a-band MIMO WLAN SoC in 45nm CMOS for multi-radio IC," in *Proceedings of IEEE International Solid-State Circuits Conference (ISSCC)*, San Francisco, CA, 2013, pp. 328-329.
- [6] O. El-Gharniti, E. Kerherve, and J. B. Begueret, "Modeling and characterization of on-chip transformers for silicon RFIC," *IEEE Transactions on Microwave Theory and Techniques*, vol. 55, no. 4, pp. 607-615, 2007.
- [7] M. Albulet, *RF Power Amplifiers*. Atlanta, GA: Noble Publishing, 2001, pp. 9-41.
- [8] O. Lee, H. Ryu, S. Baek, I. Nam, M. Jeong, and B. E. Kim, "A high-efficiency CMOS power amplifier using 2:2 output transformer for 802.11n WLAN applications," *Journal of Semiconductor Technology and Science*, vol. 15, no. 2, pp. 280-285, 2015.
- [9] S. Baek, H. Ryu, I. Nam, M. Jeong, B. E. Kim and O. Lee, "A 2.4-GHz CMOS power amplifier with parallel-combined transistors and selective adaptive biasing for wireless LAN applications," *Microwave and Optical Technology Letters*, vol. 58, no. 6, pp. 1374-1377, 2016.
- [10] T. M. Chen, W. C. Chan, C. C. Lin, J. L. Hsu, W. K. Li, P. A. Wu, et al, "A 2×2 MIMO 802.11 abgn/ac WLAN SoC with integrated T/R switch and on-chip PA delivering VHT80 256QAM 17.5 dBm in 55nm CMOS," in *Proceedings of 2014 IEEE Radio Frequency Integrated Circuits Symposium*, Tampa Bay, FL, 2014, pp. 225-228.
- [11] D. Guo, "Power amplifier and front end module requirements for IEEE 802.11n applications," *High Frequency Electronics*, vol. 10, no. 9, pp. 38-45, 2011.

Seungjun Baek



received his B.S. degree in Electrical Engineering from Pusan National University, Busan, Korea, in 2014 and his M.S. degree in Electrical engineering at Pusan National University, Busan, Korea, in 2016. His research interests are in RF power amplifier design for wireless LAN.

Hyunjin Ahn



received his B.S. degree in Electrical Engineering from Pusan National University, Busan, Korea, in 2015. He is currently working toward a PhD in electrical engineering at Pusan National University, Busan, Korea. His interests include high-frequency power amplifier design for mobile applications and low-power circuit design.

Hyunsik Ryu



received his B.S. degree in electrical engineering from Silla National University, Busan, Korea, in 2013 and M.S. degrees in Electronic and Electrical Engineering from Pusan National University, Busan, Korea in 2015. His research interests include RF power amplifier design for mobile applications, low-power RF circuit design, and active device modeling in CMOS and GaAs HBT processes.

Doo-Hyouk Choi



received his B.S. degree in Electric Wave Engineering from Kwangwoon University, Seoul, Korea, in 2008. From 2008 to 2011, he was with KCMobile, where he was involved in developing GSM cell phone RF part circuit analysis, design, and evaluation. From 2011 to 2013, he worked for the Motorola Company as an application engineer for the RF parts of smart phones. He is currently working for RAONTECH, Seongnam, Korea. His research interests are micro-display devices, wireless connectivity SoC, and mobile TV SoC using industry-leading low-power analog and RF CMOS technologies.

Ilku Nam



received his B.S. degree in EE from Yonsei University, Korea, in 1999 and M.S. and Ph.D. degrees in EECS from KAIST, Korea in 2001 and 2005, respectively. From 2005 to 2007, he was a Senior Engineer for Samsung Electronics, Suwon, Korea, where he was involved in the development of mobile digital TV tuner IC. In 2007, he joined the School of Electrical Engineering, Pusan National University, Busan, Korea, where he is a professor.

Mun-Sub Byun



received his B.S. degree in control and instrumentation engineering from Wonkwang University, Jeonbuk, Korea, in 2002 and his M.S. degree in electrical engineering from Kwangwoon University, Seoul, Korea in 2004. From 2004 to 2005, he worked for Turbotech, where he was involved in developing CDMA cell phone RF part circuit analysis, design, and evaluation. From 2005 to 2006, he was with Integrant Technologies Inc. as a senior application and field application engineer specializing in mobile TV tuners and SoC. From 2006 to 2009, he was a senior application and field application engineer for Analog Devices. From 2010 to 2011, he was at LG electronics, where he was involved in developing the circuit analysis, design, and evaluation of RF parts for CDMA cell phones. He is currently working for RAONTECH, Seongnam, Korea. His research interests are performance semiconductor package design, micro-display devices, wireless connectivity SoC, and mobile TV SoC using industry-leading low-power analog and RF CMOS technologies.

Deokgi An



received his B.S. degree and M.S. degree from Kangwon National University in Chuncheon, Korea in 2009 and 2011, respectively. In 2011, he joined RAONTECH Inc., Seongnam, Korea, where he was involved in the design and testing of CMOS RF ICs. Since 2016, he has been with Broadcom Ltd., Korea, designing RF circuits for communication systems.

Minsu Jeong



received B.S. and M.S. degrees in electrical and electronics engineering from Korea University, Seoul, Korea in 1994 and 1996, respectively. He began his career in 1997 at LG Semiconductors as an analog circuit designer. In 2002, he joined Integrant Technologies, which merged with ADI in 2006, where developed satellite DTV, DMB receivers, and Wi-Max transceivers. Recently, he moved to RAONTECH, where he is the CTO. He is now developing wireless connectivity multi-standard SoC, universal broadcasting RF receivers, and semiconductor devices for micro-display wearable devices.

Bo-Eun Kim



received his B.S., M.S., and Ph.D. degrees in electrical engineering from Korea University, Seoul, Korea in 1991, 1993, and 1997, respectively. From 1997 to 2000, he was with Hyundai Electronics, where he was involved in developing phase-locked loop ICs for memory modules. From 2000 to 2007, he was with Integrant Technologies Inc. as a co-founder and CTO, where he developed mobile TV tuners, wire-

less transceivers for high-speed communications, and RFID transceivers using CMOS technology. From 2006 to 2009, he was a product line manager for Analog Devices, Inc., which acquired Integrant Technologies Inc. In 2009, he co-founded RAONTECH Inc., where he is currently Chair and CEO. Since then he has continued his professional career in developing micro-display devices, wireless connectivity SoC, and mobile TV SoC using industry-leading low-power analog and RF CMOS technologies. His current interests include new display devices for smart glasses, head-mounted devices, and head-up display devices, which enable augmented reality and virtual reality experiences, wireless connectivity devices for wearable devices, and mobile TV SoCs that meet world TV standards using CMOS technologies. Dr. Kim is an author and coauthor of more than 40 international and domestic technical papers on analog circuits and systems. He has published more than 65 patents, both granted and pending.

Ockgoo Lee



received his B.S. degree in electrical engineering from Sungkyunkwan University, Korea in 2001, his M.S. degree in electrical engineering from KAIST, Korea in 2005, and his Ph.D. degree in electrical and computer engineering from the Georgia Institute of Technology, USA, in 2009. Upon completion of his doctorate, he joined Qualcomm Inc., USA as a Senior Engineer, where he was involved in the develop-

ment of transmitters and integrated passive circuits in mobile applications. He is currently a faculty member at the Department of Electrical Engineering, Pusan National University, Korea. His research interests include high-frequency integrated circuits and system design for wireless communica-